

# *Correlation between specific adsorption and corrosion inhibition.*

## *Adsorption of 1-butylpyridinium bromide*

L. A. AVACA, E. R. GONZÁLEZ, A. RÚVOLO FILHO\*

*Instituto de Física e Química de São Carlos, Universidade de São Paulo, CP 369, 13.560-São Carlos, SP, Brasil*

Received 20 May 1981

A correlation between specific adsorption and corrosion inhibition was made on the basis of calculations of the degree of coverage at zero charge on the electrode and corrosion rates. 1-butylpyridinium bromide (BPB) was chosen as a model compound for these studies. The electrical double-layer parameters were determined at constant charge on a mercury electrode, from values of the interfacial capacity and surface tension obtained experimentally from aqueous solutions of BPB at 25°C. The characteristics of the salt as a corrosion inhibitor were studied through Tafel plots and weight-loss measurements using mild steel plates immersed in H<sub>2</sub>SO<sub>4</sub> solutions. Analysis of the results lead to the conclusion that the salt adsorbs intensely on the metal surface, forming a complete monolayer of BP<sup>+</sup> ions in 0.1 mol dm<sup>-3</sup> solutions and multilayers for higher concentrations. The results of this work indicate that for high coverages there is a good correlation between the amount of BP<sup>+</sup> specifically adsorbed on mercury and the inhibition of the corrosion process on mild steel. That type of compound acts mainly as an anodic inhibitor in acid media by the formation of protective layers on the metal surface.

### 1. Introduction

It is well established that the characteristics of corrosion processes are closely related to the structure of the metal-solution interface and, consequently, to adsorption phenomena [1, 2]. Several works have shown that compounds containing quaternary nitrogen act as corrosion inhibitors for mild steel in acid media [3-6]. In some cases, qualitative correlations were made between the adsorption of these molecules and the mechanism of inhibition [6]. Generally, it has been argued that these compounds act mainly by blocking the metal surface affecting the hydrogen evolution reaction as well as the dissolution of the metal. This shows the importance of carrying out detailed double-layer studies on such systems.

Preliminary tests carried out in this laboratory using 1-alkylpyridinium and quinolinium halides as corrosion inhibitors in acid medium have shown that 1-butylpyridinium bromide (BPB) has an intermediate behaviour, making it a convenient choice as a model compound for adsorption studies. Ideally, the same metal as used in corrosion rate measurements should be used as the electrode material. However, the measurements of double-

layer parameters on solid metals are, in most cases, irreproducible. In contrast, data on mercury are highly reproducible and can be complemented by electrocapillary experiments. Thus, conclusions on the mechanism of inhibition would be substantiated much more if proper correlations could be made between adsorption on mercury and inhibition on other metals.

In the present work the specific adsorption of BPB is studied on mercury through the measurement of the differential capacity of the interface. The results are correlated with corrosion data obtained by weight-loss measurements and polarization curves on mild steel in acid solutions containing BPB.

### 2. Experimental procedure

1-butylpyridinium bromide was synthesized by refluxing a mixture of pyridine and *n*-butyl bromide which was then purified by six recrystallizations from acetone at 40°C. The absence of impurities was checked by gas chromatography. AR grade materials were used throughout. Water and mercury were purified in the usual way [7] for electrochemical work.

\* Permanent address: Departamento de Química, Universidade Federal de São Carlos, Brasil.

A detailed account of the experimental system used for the measurement of the differential capacity of the mercury-solution interface and the potential of zero charge ( $E_z$ ) has been reported elsewhere [7]. The capacities were found to be independent of frequency in the range 50–800 Hz. The values of the interfacial tension at a potential of zero charge ( $\gamma_z$ ) were obtained by measuring the drop time in the corresponding solutions and in a 0.95 mol dm<sup>-3</sup> NaF solution [8] used as a standard to establish the proportionality constant. The drop time measurements were carried out using a special cell with flat glass windows and an optical-electronic system developed in this laboratory. In this system, the drop interrupts a light beam between a source and a phototransistor (GE Photo Darlington 2N5777) generating a 5-V pulse which activates a Timer HP 5326B. An average of 50 drop time measurements for each concentration of BPB resulted in a reproducibility of 1 ms.

Corrosion rates were determined by gravimetric measurements on 2 mm thick mild steel plates of 2 cm<sup>2</sup> total exposed area, immersed in 250 cm<sup>3</sup> of the corroding solution for 2 h. Deoxygenation was accomplished when necessary with purified nitrogen. Rest potentials and polarization curves were obtained in a three-compartment cell having a 0.3 cm<sup>2</sup> area mild steel working electrode, a platinum counter and a saturated calomel electrode (SCE) as reference. The mild steel working electrode was mounted in an appropriate nylon support. Its percentage composition was determined as being: 0.18 C, 0.24 Si, 0.37 Mn, 0.010 P, 0.016 S.

All electrochemical measurements were carried out using a PAR Mod. 170 Electrochemical System. Potentials are all referred to the SCE. In all cases the temperature was maintained at 25 ± 0.2° C.

### 3. Results

#### 3.1. Adsorption of BPB on mercury

Figure 1 shows the differential capacity as a function of the electrode potential for mercury-aqueous BPB solution systems at concentrations varying within the range 0.01 to 0.5 mol dm<sup>-3</sup> and for potentials in the range -0.1 to -0.9 V. The cathodic limit was imposed by the fact that BPB

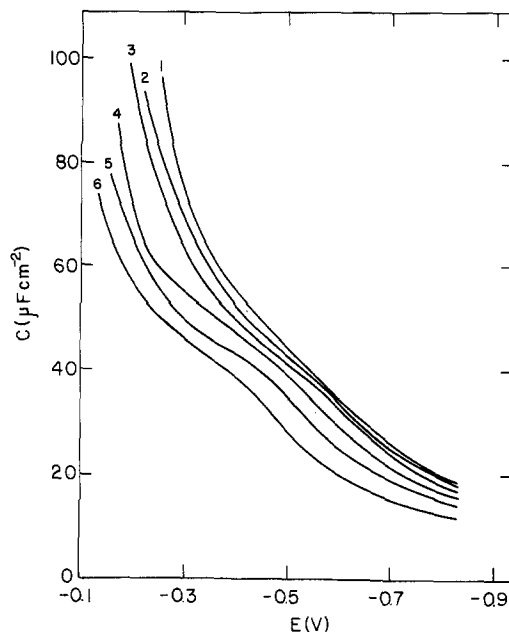


Fig. 1. Differential capacity of the electrical double-layer for a mercury electrode in aqueous BPB solutions at 25° C. [BPB] in mol dm<sup>-3</sup>: (1) 0.5; (2) 0.2; (3) 0.1; (4) 0.05; (5) 0.025; (6) 0.010.

suffers electrochemical reduction at more negative potentials. At the anodic end, all the curves showed large, frequency-dependent peaks probably related to a desorption process as reported for analogous systems [2]. A characterization of those peaks is beyond the scope of this work since they are well outside the potential region where a correlation between corrosion rate and adsorption is meaningful. For this reason, the peaks are not included in Fig. 1 and will not be considered in the subsequent calculations.

The values of  $E_z$  and  $\gamma_z$  measured for different solutions of BPB are presented in Table 1. The data in Table 1 were used to calculate the double-layer parameters through appropriate theoretical relationships and the use of a computer program.

Table 1. Electrocapillary data for aqueous solutions of BPB at 25° C

| [BPB] (mol dm <sup>-3</sup> ) | $E_z$ (V) | $\gamma_z$ (mN m <sup>-1</sup> ) |
|-------------------------------|-----------|----------------------------------|
| 0.010                         | -0.4370   | 328.30                           |
| 0.025                         | -0.4578   | 320.72                           |
| 0.05                          | -0.4724   | 313.41                           |
| 0.1                           | -0.4838   | 306.62                           |
| 0.2                           | -0.4971   | 292.60                           |
| 0.5                           | -0.5164   | 271.60                           |

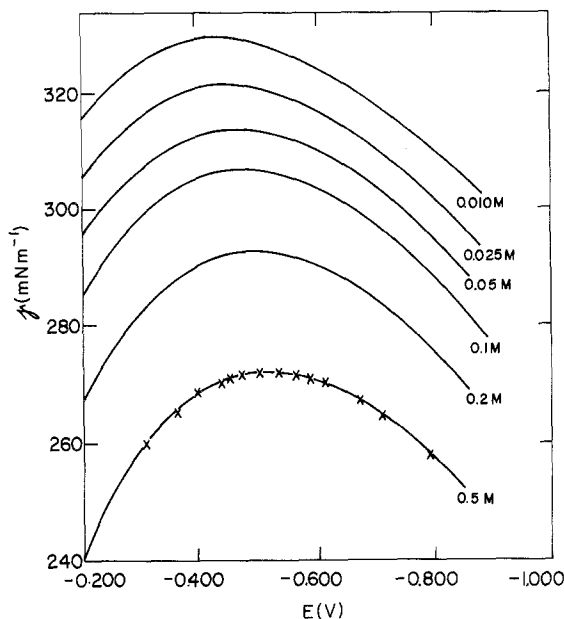


Fig. 2. Electrocapillary curves for mercury-aqueous BPB solution systems at 25°C obtained from computer integration. X: experimental data for 0.5 mol dm<sup>-3</sup> BPB solution.

Initially, the capacity-potential data were integrated from  $E_z$  to obtain the charge density on the electrode ( $q^m$ ).

A second integration using  $\gamma_z$  as the constant led to the electrocapillary curves shown in Fig. 2. A complete electrocapillary curve, recorded experimentally for the 0.5 mol dm<sup>-3</sup> solution, was found to be coincident within experimental error with the one obtained by double integration of the corresponding capacity curve.

A comparison of the curves in Fig. 2 with those obtained in KBr solutions [9] shows that on top of the adsorption of the anion there is a very strong contribution from the cation, similar to that already observed for the tetraalkylammonium ions [10].

With the values of  $\gamma$  and  $q^m$ , the Parsons functions  $\xi_{\pm} = q^m E_{\pm} + \gamma$  were calculated after converting the  $E$  scale into one of thermodynamic significance [11]. As the activity coefficients for BPB are not available it was assumed that those reported for tetrabutylammonium bromide [12] could approximate the behaviour of the present system. The Parsons function  $\xi_{-}$  was differentiated at constant  $q^m$  with respect to the chemical potential of the salt to obtain the total adsorbed

charge density due to cations ( $q_{+}$ ). The corresponding value for the anions ( $q_{-}$ ) was obtained from  $q^m$  by applying the electroneutrality condition.

A rigorous separation of those charges into contributions from the specifically adsorbed charge and diffuse layer charge, for both anion and cation, would require an extensive set of measurements which is beyond the scope of this work. Thus, in order to estimate the charge due to anions in the diffuse layer it was assumed [10] that the specifically adsorbed charge due to bromide ions is the same as that measured in pure KBr solutions [9]. This assumption allows the direct calculation of the anion diffuse layer charge ( $q_{-}^{2-s}$ ) and, through the Gouy-Chapman theory, of the cation diffuse layer charge ( $q_{+}^{2-s}$ ). With this value, the specifically adsorbed charge due to cations ( $q_{+}^1$ ) follows directly. Figure 3 shows  $q_{+}^1$  as a function of  $q^m$  for the different concentrations of BPB.

### 3.2. Effect of BPB on corrosion rate

Anodic-cathodic polarization curves for mild steel electrodes were obtained in aqueous 0.2 mol dm<sup>-3</sup> Na<sub>2</sub>SO<sub>4</sub> solutions at pH = 2.0, adjusted by addition of H<sub>2</sub>SO<sub>4</sub>, and containing BPB in variable

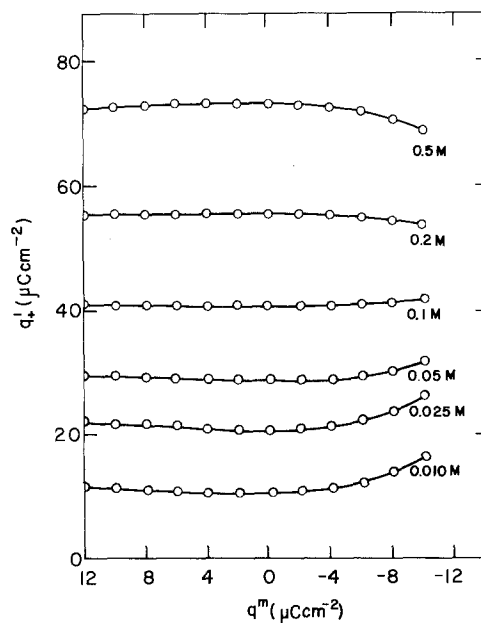


Fig. 3. Charge due to specifically adsorbed cations for mercury-aqueous BPB solution systems at 25°C as a function of the charge on the metal.

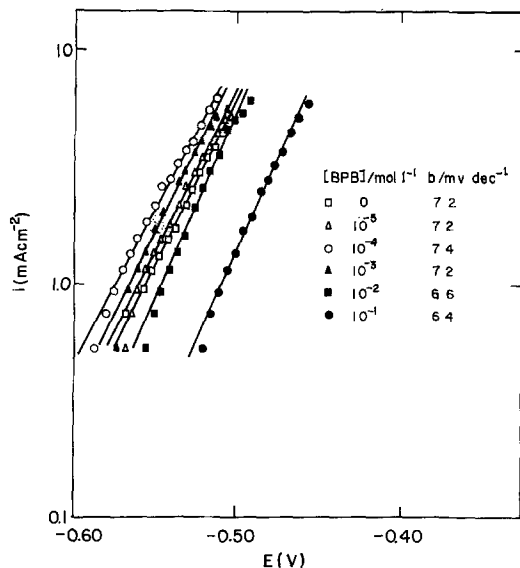


Fig. 4. Anodic Tafel plots for mild steel – 0.2 mol dm<sup>-3</sup> aqueous Na<sub>2</sub>SO<sub>4</sub> solution systems containing variable amounts of BPB at 25°C and pH = 2.0. Values of the slope (*b*) are indicated for each concentration of BPB.

amounts. Figure 4 shows the corresponding anodic Tafel plots while Table 2 presents the zero-current potential values obtained from the curves. The rest potentials measured at open circuit for each solution are also included in Table 2.

Corrosion rates for mild steel in 1 mol dm<sup>-3</sup> H<sub>2</sub>SO<sub>4</sub> were determined through the weight-loss of suitable specimens as described already. The values obtained as a function of the concentration of BPB can be readily converted into corrosion current densities by assuming that the dissolution reaction involves two Faradays per mole. The results obtained are presented in Fig. 5, where the rest-potential values are also plotted in order to

Table 2. Rest potentials ( $E_R$ ) and zero-current potentials ( $E_{i=0}$ ) for mild steel in aqueous solutions of Na<sub>2</sub>SO<sub>4</sub> 0.2 mol dm<sup>-3</sup>, containing variable amounts of BPB, pH = 2.0

| [BPB] (mol dm <sup>-3</sup> ) | $E_R$ (V) | $E_{i=0}$ (V) |
|-------------------------------|-----------|---------------|
| 0                             | -0.600    | -0.605        |
| 10 <sup>-5</sup>              | -0.595    | -0.590        |
| 10 <sup>-4</sup>              | -0.605    | -0.610        |
| 10 <sup>-3</sup>              | -0.590    | -0.585        |
| 10 <sup>-2</sup>              | -0.580    | -0.575        |
| 10 <sup>-1</sup>              | -0.540    | -0.540        |

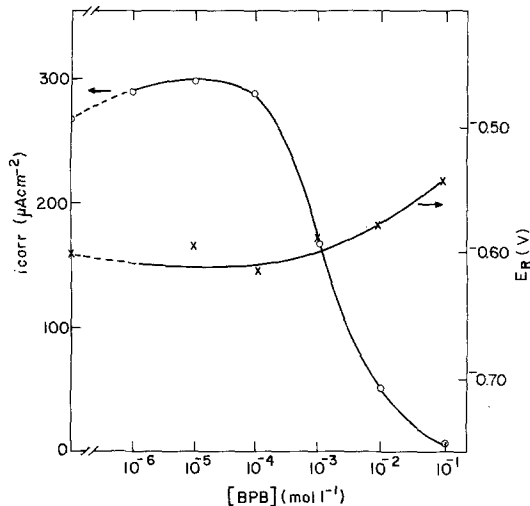


Fig. 5. Rest potentials,  $E_R$ , and calculated corrosion current density,  $i_{corr}$ , for mild steel in 1 mol dm<sup>-3</sup> H<sub>2</sub>SO<sub>4</sub> as a function of the inhibitor concentration.

correlate the behaviour of the two functions better. For concentrations of BPB above 0.1 mol dm<sup>-3</sup> the weight losses were negligible.

#### 4. Discussion

An analysis of the electrocapillary curves (Fig. 2) shows that for 0.01 mol dm<sup>-3</sup> solutions the value of  $\gamma_z$  for BPB is 98 mN m<sup>-1</sup> lower than for KBr [9]. This demonstrates the strong adsorption of the BP<sup>+</sup> cation on mercury, which is even larger than that reported for the tetraalkylammonium cations [10].

It is interesting to note that although the cation is much more strongly adsorbed than the bromide ion, the shift of  $E_z$  with concentration (Table 1) is increasingly negative. This unexpected behaviour is probably due to the fact that the specific adsorption of the BP<sup>+</sup> cations shows little dependence on the electrode charge (Fig. 3) while for bromine ions that dependence is appreciable [9].

The variations of the specifically adsorbed charge due to cations with the electrode charge for different concentrations of BPB (Fig. 3), shows that in the interval  $12 > q^m > -6 \mu\text{C cm}^{-2}$ ,  $q_1^+$  is almost independent of  $q^m$ . This means that, for a given concentration, the chemical interactions between the metal surface and the substrate are predominant even with positive charges on the

Table 3. Degree of coverage for a mercury electrode at  $q^m = 0 \mu\text{C cm}^{-2}$ , for different concentrations of BPB in water at  $25^\circ\text{C}$

| [BPB] ( $\text{mol dm}^{-3}$ ) | $q_+^1$ ( $\mu\text{C cm}^{-2}$ ) | $q_+^1$ ( $\mu\text{C cm}^{-2}$ ) | Degree of coverage |
|--------------------------------|-----------------------------------|-----------------------------------|--------------------|
| 0.1                            | -5.1                              | 40.26                             | 0.77               |
| 0.2                            | -8.0                              | 55.20                             | 1.06               |
| 0.5                            | -10.5                             | 73.0                              | 1.41               |

electrode. On the other hand, these constant values of  $q_+^1$  are dependent on the concentration of BPB (which determines the ionic strength of the solution) due to the strong influence of imaging in the diffuse layer.

For concentrations of BPB below  $0.1 \text{ mol dm}^{-3}$ , the amount of specifically adsorbed cations increases for  $q^m < -6 \mu\text{C cm}^{-2}$ , showing that the electrostatic interactions with the electrode become important at sufficiently negative charges. In contrast, the opposite effect is observed for higher concentrations.

In order to explain this peculiar behaviour of the system, a calculation of the degree of coverage at  $q^m = 0$  was carried out assuming a model for the adsorbed particles in which the aromatic ring lies flat on the surface. Thus, the area of a BPB<sup>+</sup> cation was calculated as being  $0.29 \text{ nm}^2$ , while for Br<sup>-</sup> a value of  $0.12 \text{ nm}^2$  was used. Table 3 shows that for concentrations higher than  $0.1 \text{ mol dm}^{-3}$  the structure of the double layer can only be described assuming the formation of multilayers. Under these conditions, extra amounts of cations can enter the inner layer assisted by adsorbed anions. This phenomenon has been reported also for the adsorption of tetraalkylammonium salts [1, 2].

When the charge on the electrode becomes negative enough, anions are repelled from the surface leaving behind only a monolayer of adsorbed cations. This explains the decrease of  $q_+^1$  at the most negative charges for concentrated solutions.

The analysis above would also justify the convergence of the curves of Fig. 3 to a common value of  $q_+^1$  of around  $45 \mu\text{C cm}^{-2}$  at  $q^m = -15 \mu\text{C cm}^{-2}$ , which corresponds to 0.82 of a close-packed monolayer of cations, which is a reasonable value for an actual monolayer.

An examination of Fig. 5 shows the existence of two regions in which the effect of BPB on the corrosion rate is opposite. For BPB concentrations

up to  $10^{-4} \text{ mol dm}^{-3}$  the corrosion current increases slightly and, at the same time, the rest potential shifts cathodically. As shown by the Tafel plots (Fig. 4), the anodic process is effectively accelerated under these conditions accounting for the observed shift in  $E_r$ . The adsorption studies showed that at those concentrations of BPB the degree of coverage must be very low so the acceleration of the anodic reaction must be attributed to the stabilization of Fe(II) by the bromide ions in solution.

At the other extreme of the concentration range ( $10^{-1} \text{ mol dm}^{-3}$ ) the degree of coverage tends to unity and, at the same time a marked inhibition of the anodic process can be observed from Fig. 4. Under these conditions, the corrosion current drops from a value of near  $300 \mu\text{A cm}^{-2}$  to a negligible value of  $4 \mu\text{A cm}^{-2}$  while the rest potential shows a noticeable shift towards more noble potentials. These observations indicate that for high coverages there is a good correlation between the amount specifically adsorbed on mercury and the inhibition of the corrosion process in mild steel. So it might be concluded that this type of compound acts as an anodic inhibitor in acid media by the formation of protective layers on the metal surface.

However, for intermediate concentrations (e.g.  $10^{-2} \text{ mol dm}^{-3}$ ) it is not possible as yet to establish quantitative correlations since an almost six-fold drop in the corrosion rate is observed with a degree of coverage of only 20%. This shows the necessity of further studies leading to the establishment of an alternative model for the inhibition mechanism.

#### Acknowledgements

The authors wish to thank the Conselho Nacional de Desenvolvimento Científico e Tecnológico (CNPq), Brasil, for financial support.

**References**

- [1] J. B. Hayter and R. J. Hunter, *J. Electroanal. Chem.* **37** (1972) 71.
- [2] J. B. Hayter and R. J. Hunter, *J. Electroanal. Chem.* **37** (1972) 81.
- [3] T. P. Hoar and R. D. Holliday, *J. Appl. Chem.* **3** (1953) 502.
- [4] J. M. West, *J. Appl. Chem.* **10** (1960) 250.
- [5] R. J. Meakins, *Australasian Corrosion Engineering* **11** (1967) 5.
- [6] K. Chandrasekhara Pillar and R. Narayan, *J. Electrochem. Soc.* **125** (1978) 1393.
- [7] E. R. González, *J. Electroanal. Chem.* **90** (1978) 431.
- [8] A. W. M. Ver kroost, M. Sluyters-Rehbach and J. H. Sluyters, *J. Electroanal. Chem.* **24** (1970) 1.
- [9] J. Lawrence, R. Parsons and R. Payne, *J. Electroanal. Chem.* **16** (1968) 193.
- [10] M. A. V. Devanathan and M. J. Fernando, *Trans. Faraday Soc.* **58** (1962) 368.
- [11] P. Delahay, 'Double Layer and Electrode Kinetics', Wiley-Interscience, New York (1965) p. 54.
- [12] J. V. Leyendekkers and R. J. Hunter, *J. Electroanal. Chem.* **81** (1977) 123.